



LJMU Research Online

Gonzalez, JA, Ogba, OM, Morehouse, GF, Rosson, N, Houk, KN, Leach, AG, Cheong, PH-Y, Burke, MD and Lloyd-Jones, GC

MIDA boronates are hydrolysed fast and slow by two different mechanisms.

<http://researchonline.ljmu.ac.uk/id/eprint/4716/>

Article

Citation (please note it is advisable to refer to the publisher's version if you intend to cite from this work)

Gonzalez, JA, Ogba, OM, Morehouse, GF, Rosson, N, Houk, KN, Leach, AG, Cheong, PH-Y, Burke, MD and Lloyd-Jones, GC (2016) MIDA boronates are hydrolysed fast and slow by two different mechanisms. Nature Chemistry, 8 (11). pp. 1067-1075. ISSN 1755-4330

LJMU has developed **LJMU Research Online** for users to access the research output of the University more effectively. Copyright © and Moral Rights for the papers on this site are retained by the individual authors and/or other copyright owners. Users may download and/or print one copy of any article(s) in LJMU Research Online to facilitate their private study or for non-commercial research. You may not engage in further distribution of the material or use it for any profit-making activities or any commercial gain.

The version presented here may differ from the published version or from the version of the record. Please see the repository URL above for details on accessing the published version and note that access may require a subscription.

For more information please contact researchonline@ljmu.ac.uk

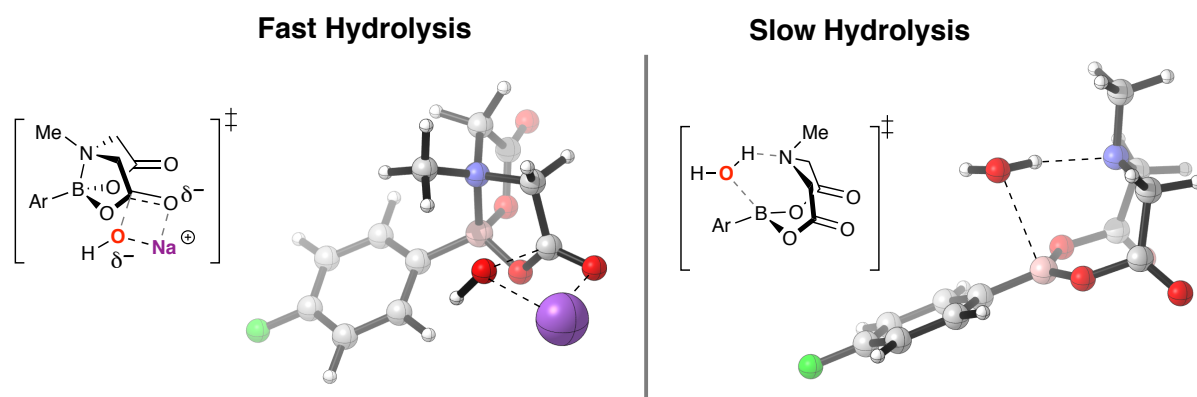
<http://researchonline.ljmu.ac.uk/>

MIDA boronates are hydrolysed fast and slow by two different mechanisms

Jorge A. Gonzalez,^a O. Maduka Ogba,^b Gregory F. Morehouse,^c Nicholas Rosson,^b
Kendall N. Houk,^d Andrew G. Leach,^e Paul H.-Y. Cheong,^{b*}
Martin D. Burke,^{c*} and Guy C. Lloyd-Jones^{a*}

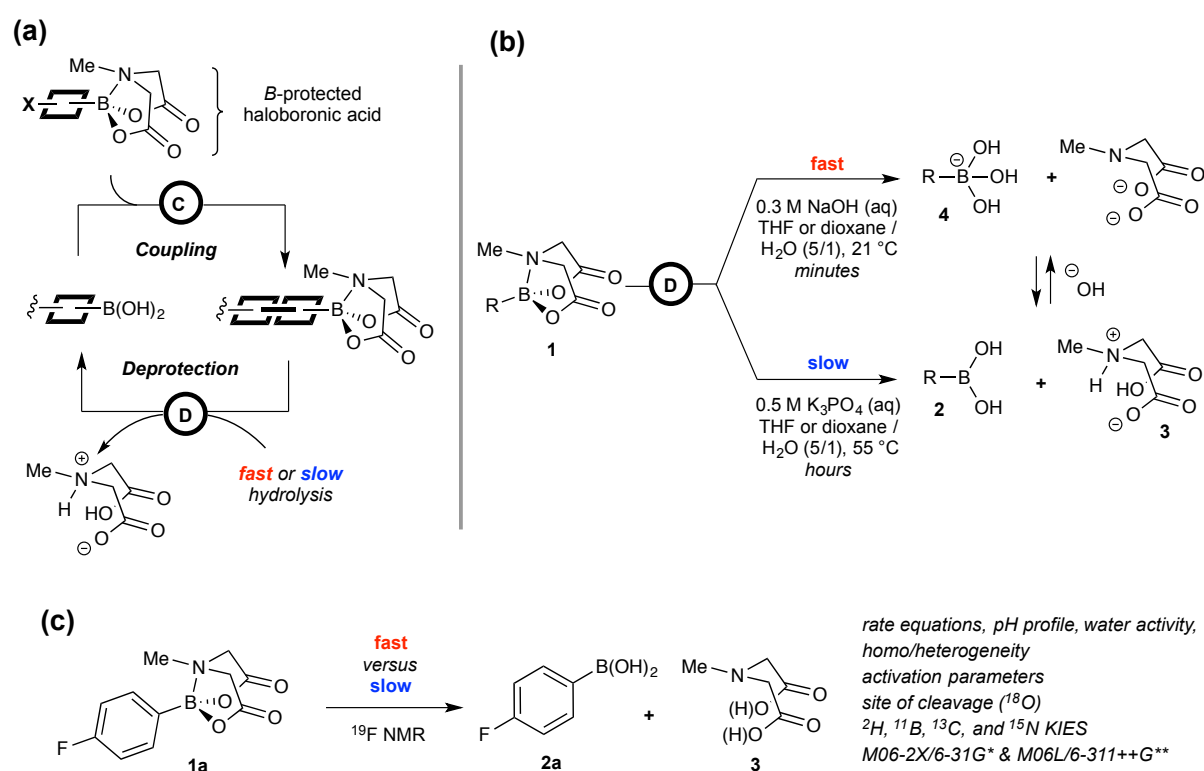
- a) EaStCHEM, School of Chemistry, University of Edinburgh, Edinburgh, EH9 3FJ, UK
b) Department of Chemistry, Oregon State University, Corvallis, OR 97331, USA
c) Department of Chemistry University of Illinois 454 RAL, Box 52-5 600 South Mathews Avenue Urbana, IL 61801, USA
d) Department of Chemistry and Biochemistry, University of California, Los Angeles, 607 Charles E. Young Drive East, Los Angeles, CA 90095-1569, USA
e) School of Pharmacy and Biomolecular Sciences, Liverpool John Moores University, Byrom Street, Liverpool, L3 3AF, UK

*e-mail: paulc@science.oregonstate.edu,
mdburke@illinois.edu
and guy.lloyd-jones@ed.ac.uk



MIDA boronates serve as an increasingly general platform for building-block-based small molecule construction, largely due to the dramatic and general rate differences with which they are hydrolysed under various basic conditions. Yet the mechanistic underpinnings of these rate differences have remained unclear, hindering efforts to address current limitations of this chemistry. We have now identified two distinct mechanisms for hydrolysis: 'base-mediated' and 'neutral'. The former can proceed more than three orders of magnitude faster, and involves rate-limiting attack at a MIDA carbonyl carbon by hydroxide. The alternative 'neutral' hydrolysis does not require an exogenous acid/base and involves rate-limiting B-N bond cleavage by a small water cluster, (H₂O)_n. The two mechanisms can operate in parallel, and their relative rates are readily quantified by ¹⁸O incorporation. Whether hydrolysis is 'fast' or 'slow' is dictated by the pH, the water activity (a_w), and mass-transfer rates between phases. These findings stand to rationally enable even more effective and widespread utilisation of MIDA boronates in synthesis.

1 *N*-Methylimidodiacetic acid esters (**1**) of boronic acids (**2**) (“MIDA boronates”) have
 2 emerged as an increasingly general and automated platform for building-block-based small
 3 molecule synthesis,¹ Figure 1. One of the most important and yet poorly understood features
 4 that enable such utility is distinct rates of hydrolysis for MIDA boronates under various basic
 5 conditions.^{2,3} When ethereal solutions of MIDA boronates are treated with aqueous NaOH,
 6 they are hydrolysed within minutes at room temperature,² whereas with aqueous K₃PO₄, slow
 7 hydrolysis take several hours at elevated temperatures.³ When performing cross-couplings of
 8 boronic acids in the presence of anhydrous K₃PO₄, MIDA boronates undergo little or no
 9 hydrolysis, even though small amounts of water are presumably formed via boronic acid
 10 oligomerisation.²



11

12 **Figure 1 | Hydrolytic Deprotection and Coupling of MIDA boronates.** (a) Schematic representation of
 13 iterative coupling platform for small molecule synthesis from MIDA boronate building blocks; (b) Deprotection
 14 of MIDA boronates **1** via 'fast' and 'slow' hydrolysis. $k_{\text{REL}} \approx 3.5 \times 10^4$ at 21 °C in a homogeneous medium of THF
 15 / H₂O (5 / 1, approx. 9.3 M H₂O); (c) reaction system selected for mechanistic investigation.

16

17 In contrast to other boronates,⁴ MIDA hydrolysis rates are remarkably insensitive to the
 18 structure of the organic fragment,^{2,3} and this generality has enabled these dramatic rate
 19 differences to be harnessed to great effect. The lack of hydrolysis under conditions that
 20 promote cross-coupling, combined with fast hydrolysis by NaOH, collectively enable

1 iterative synthesis of small molecules from a wide range of halo-MIDA boronate building
2 blocks in a manner analogous to iterative peptide coupling.^{2,5} Harnessing this approach, many
3 different types of natural products (including highly complex macrocyclic and polycyclic
4 structures), biological probes, pharmaceuticals, and materials components have now been
5 prepared using just one reaction iteratively.¹ A machine has also been created that can
6 execute such building-block-based small molecule construction in a fully automated fashion.⁶
7 With suitably active catalysts, slow hydrolysis of MIDA boronates can release boronic acids
8 at a rate that avoids their accumulation during cross-coupling. Using this approach,
9 substantial improvements in yields have been achieved using MIDA boronates as stable
10 surrogates for unstable boronic acids,³ including the notoriously unstable but very important
11 2-pyridyl systems.⁷ Careful modulation of the extent of base hydration can also be used to
12 control hydrolysis and thus speciation in mixtures of boron reagents, allowing selective cross-
13 coupling followed by MIDA redistribution.⁸ Collectively, these findings have provided
14 substantial momentum towards a general and automated approach for small molecule
15 synthesis.

16 Understanding the mechanism(s) by which these distinct rates of hydrolysis occur is critical,
17 however, for addressing several current limitations of this platform and thereby maximising
18 its generality and impact. Iterative cross-couplings with more challenging Csp^2 centers that
19 are performed at higher temperatures and/or longer reaction times can be accompanied by
20 undesired MIDA hydrolysis and thus suboptimal yields. Generalised iterative couplings with
21 sp^3 hybridised carbon and heteroatoms would be highly enabling,^{9,10} but such reactions can
22 require even more forcing conditions, causing extensive MIDA hydrolysis. Executing
23 iterative cross-coupling-based syntheses requires access to complex boron-containing
24 building blocks, and doing so from simpler MIDA boronate starting materials plays an
25 important role in this process.¹¹ However, such transformations can also be hindered by
26 competitive hydrolysis during various reactions, work-ups, and/or purifications. MIDA
27 boronate hydrolysis under various mixed-phase HPLC conditions can also hinder analysis.
28 Finally, transitioning this iterative cross-coupling platform to a flow chemistry format would
29 open up many additional opportunities, and the capacity for bifunctional building blocks to
30 tolerate aqueous basic cross-coupling conditions would substantially facilitate this transition.
31 For all of these reasons, an even more stable iminodiacetic acid (**3**) motif would be highly
32 impactful. There are also cases where a more rapidly hydrolysing boronate would be
33 preferred. For example, to enable iterative boron-selective reactions with polyborylated

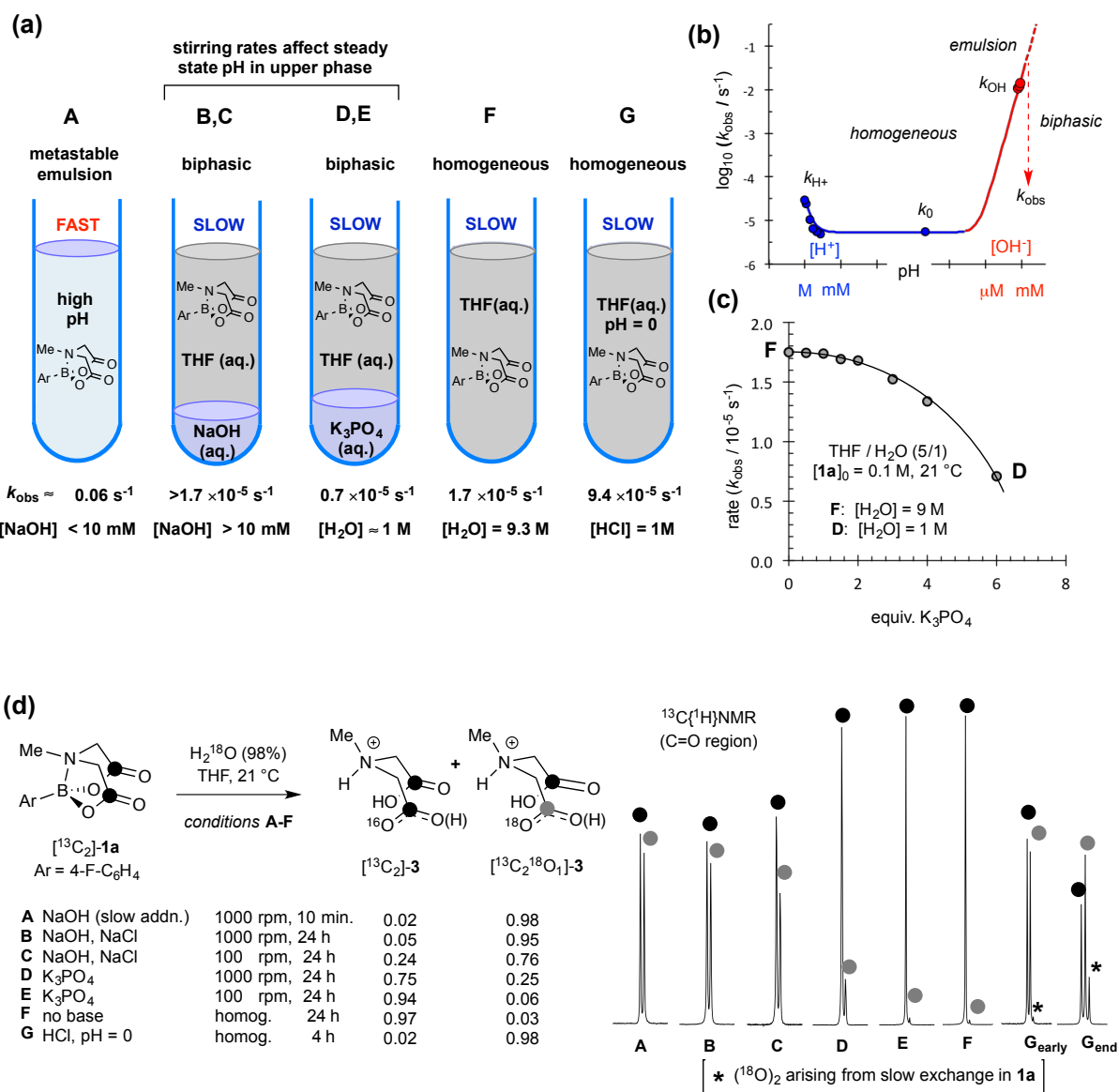
1 intermediates and tuning of slow-release conditions to optimise cross-couplings with some of
2 the most challenging partners. Finally, we have noted that when exposed to aqueous-ethereal
3 NaOH some MIDA boronates initially hydrolyse rapidly and then relatively slow, requiring
4 extended reaction times for complete hydrolysis. Eliminating such effects would substantially
5 enable efforts towards faster and more generalised automation. For all of these reasons, we
6 set out to understand the mechanism(s) by which MIDA boronates hydrolyse, both fast and
7 slow.

8 **Results**

9 1. *Distinction of limiting mechanisms for 'fast' and 'slow' release.* After preliminary tests with
10 alkyl and aryl MIDA boronates, we focussed on **1a** (Figure 1c) using *in situ* ^{19}F NMR to
11 analyse a range of hydrolysis conditions (**A** to **G**, Figure 2a). We began by study of 'fast
12 release'² (conditions **A**), where a key aspect is the heterogeneity of the medium: slow
13 addition of aq. NaOH generates a metastable emulsion. However, if addition rates are too fast
14 and $[\text{NaOH}]$ rises above 10mM, phase-separation begins to occur. Full phase-separation leads
15 to precipitous reductions in hydrolysis rates ($\sim 10^{-3}$; conditions **B**, **C**).

16 The 'slow release' conditions,³ (aq. K_3PO_4 , 7.5 equiv.) rapidly induce full phase-separation,
17 with less than 3% hydrolysis of **1a** occurring prior to this, irrespective of the stirring rate
18 (conditions **D**, **E**). Hydrolysis of **1a** proceeds in the absence of any exogenous base
19 (conditions **F**) and does so faster than under 'slow release' conditions. This phenomenon
20 arises from the partial dehydration of the organic phase by the K_3PO_4 (compare conditions **D**
21 and **F**, Figure 2c).

22 We also tested strongly acidic conditions ($\text{pH} = 0$, conditions **G**) but these only induce
23 modest rate accelerations (less than 5-fold). Three distinct hydrolytic regimes (Figure 1b)
24 were thus identified: acid (k_{H^+}), neutral (k_0) and basic (k_{OH}).



1

2 **Figure 2 | Distinction of limiting pathways for basic (fast, A), neutral (slow, F) and acidic (G) hydrolysis of 1a.**
 3 **(a)** Schematic representation of conditions A-G; **(b)** pH rate profile; autoprotolysis constant estimated (0.5
 4 mol-fraction THF) as $pK_{\text{app}} = 20$. Hydrolysis of water-soluble Me-B(MIDA) in aqueous buffer (pH 1-11) confirms
 5 $k_{\text{obs}} = k_{\text{H}^+}[\text{H}^+] + k_0 + k_{\text{OH}}[\text{OH}^-]$. **(c)** Impact of K₃PO₄ on hydrolysis rate under *heterogeneous* conditions with
 6 vigorous stirring. Line through data is an aid to the eye. **(d)** ¹³C{¹H}NMR Sub-spectra (178.70-178.85 ppm;
 7 $\Delta\delta_{\text{C}}^{18\text{O}/16\text{O}} = 30$ ppb) of MIDA ligand (3) from hydrolysis of [¹³C₂]-1a in THF/¹⁸OH₂ under conditions A to G; in
 8 acid there is slow ¹⁸O exchange in 1a (G_{early}:25% conversion, G_{end}:>98 % conversion). For all other conditions:
 9 no exchange in 1a, and very slow ¹⁸O exchange in 3 ($\leq 1.4\%$, 48 h).

10

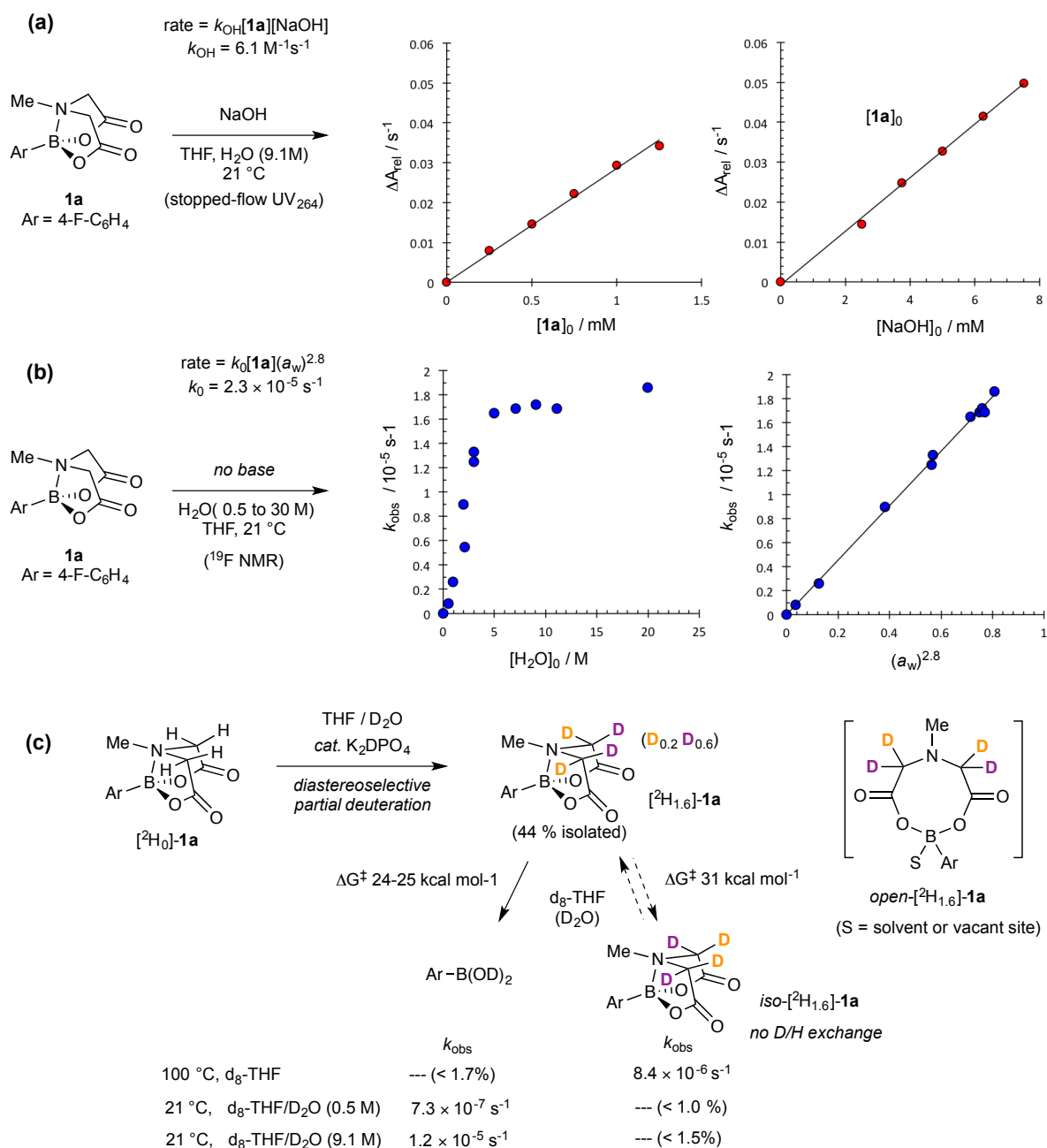
11 Further insight came from ¹³C{¹H} NMR analysis of the MIDA ligand liberated by
 12 hydrolysis of [¹³C₂]-1a in THF/H₂¹⁸O (9.1 M), Figure 2d. Two distinct reactivity patterns
 13 emerged: under basic or acidic homogeneous conditions (A and G), hydrolysis leads to mono
 14 ¹⁸O-incorporation, whereas under neutral conditions (F) there is no significant ¹⁸O-
 15 incorporation. For conditions B to E, intermediate between strongly basic and neutral, a

1 quantifiable transition between the two outcomes is evident. Importantly, it can be seen that
2 'slow-release' with K_3PO_4 (conditions **D**, **E**) predominantly, but not exclusively, proceeds via
3 neutral hydrolysis, with mixing efficiency dictating base transport rates into the upper organic
4 phase, and in turn, the extent of ^{18}O -incorporation (6%-25%).

5 In the context of MIDA boronate hydrolysis for cross-coupling,^{2,3} there are thus two
6 competing processes to consider: neutral (k_0) and basic (k_{OH}). Base-mediated hydrolysis is by
7 far the fastest ($>10^3$ fold), provided that an emulsive state is attained by vigorous agitation
8 during dispersive slow-addition of the NaOH. These conditions result in C-O cleavage in just
9 one of the two esters in **1a**, as identified by single ^{18}O incorporation in **3**. Neutral hydrolysis
10 solely cleaves [B-OC(O)] bonds, resulting in no ^{18}O incorporation in **3** at all.

11 2. *Rate laws for basic (k_{OH}) and neutral (k_0) hydrolysis.* The kinetics of 'fast-release' (k_{OH}),
12 were determined by UV at low reactant concentrations using stopped-flow techniques, Figure
13 3a. The data are indicative of rate-limiting attack by a single hydroxide (rate =
14 $k_{OH}[\mathbf{1a}][NaOH]$; $k_{OH} = 6.1 \text{ M}^{-1} \text{ s}^{-1}$) with **1a** being similarly reactive to a *p*-NO₂-benzoate
15 ester.¹² A linear free energy relationship for k_{OH} was established across a series of
16 ArB(MIDA) substrates. In the context of attack by hydroxide, the relative insensitivity of the
17 aromatic ring ($\log(k_X/k_H) = 0.5\sigma$) weighs strongly against a pathway involving rate-limiting
18 generation of a boronate anion. The acid catalysed pathway (Figure 2, **G**) is even less
19 sensitive to aryl substitution, $\log(k_X/k_H) \leq 0.01\sigma$.

20 The kinetics of neutral hydrolysis (k_0) were measured across a wide range of water
21 concentrations (0.5 to 20 M). Clean pseudo first-order decays in **1a** (k_{obs} , s^{-1}) were observed
22 in all cases, however, despite the hydrolysis being 'slow', determination of an overall rate law
23 was not straightforward, Figure 3b.



1

2 **Figure 3 | Kinetics of fast and slow hydrolysis of MIDA boronate 1a.** (a) Homogeneous basic conditions
 3 analysed by stopped-flow UV ($\Delta A_{264} / \text{s}^{-1}$). Oxidation¹¹ of nascent **2a** to the phenol (4-F-C₆H₄OH) is accounted
 4 for in the analysis, see supporting information. (b) Homogeneous neutral conditions, analysed by ¹⁹F NMR.
 5 Hydrolysis rates correlate with water activity, $k_0 = k'(a_w)^{2.8}$; $k' = 2.3 \times 10^{-5} \text{ s}^{-1}$, 21 °C. As hydrolysis proceeds,
 6 nascent zwitterion **3** either precipitates from solution ($[\text{H}_2\text{O}] \leq 3 \text{ M}$), or induces minor phase-separation.
 7 Control experiments confirmed these phenomena had negligible impact on rates. (c) Tests (negative) for "open
 8 **1a**" under conditions of homogeneous neutral hydrolysis.

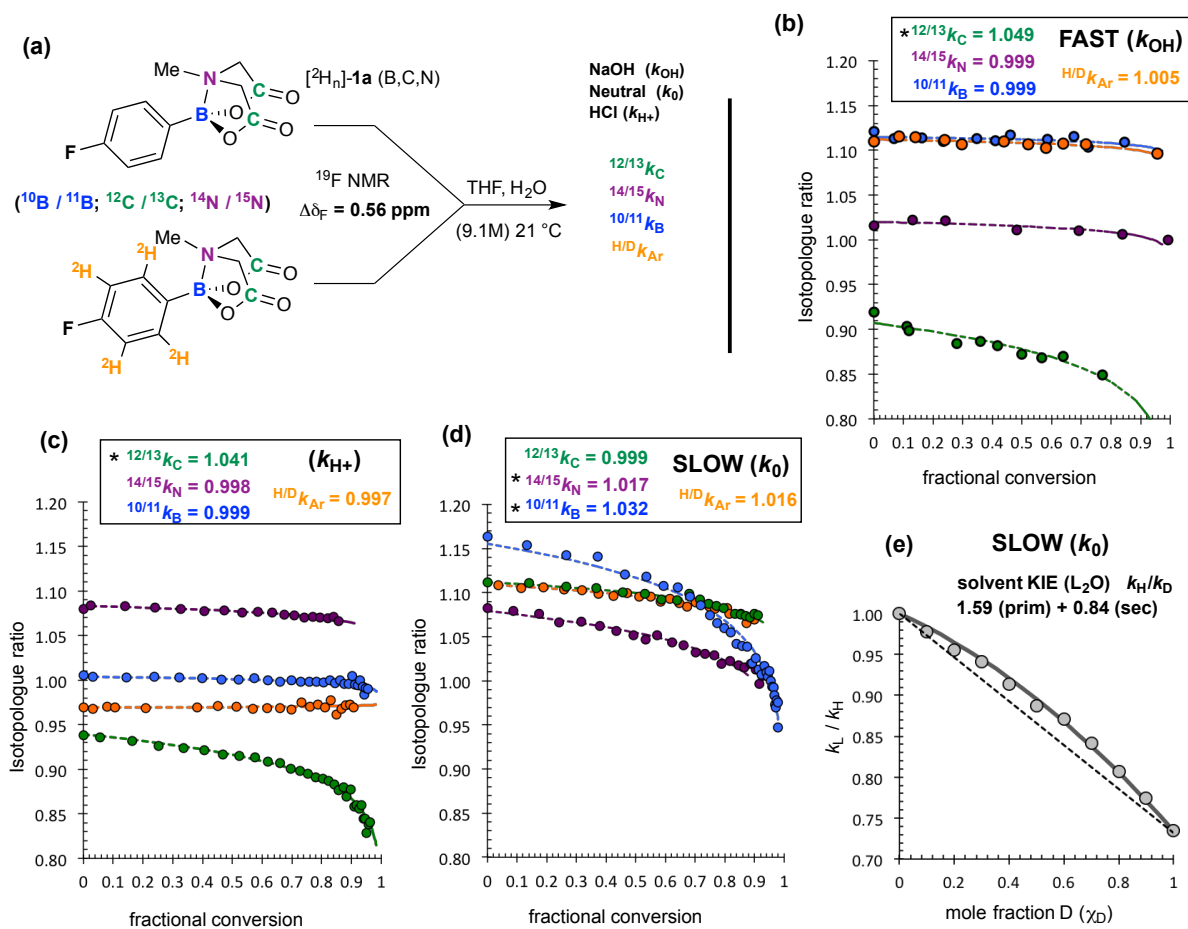
9

10 Analysis of k_{obs} as a function of water concentration gave a profile in which there is a rate-
 11 plateau, suggestive of a change in rate-limiting step, as might occur if pre-dissociation of the
 12 B-N bond in **1a**, to give a reactive "open-**1a**" intermediate was involved. However, this was
 13 not consistent with the entropy of activation ($\Delta S^\ddagger = -16 \text{ cal K}^{-1} \text{ mol}^{-1}$, 9.0 M H₂O) and tests

1 for "open-**1a**", using diastereoselectively deuterated [²H_{1.6}]-**1a**, were negative (Figure 3c).
2 Indeed, [²H_{1.6}]-**1a** required heating to 100 °C before significant rates of interconversion with
3 *iso*-[²H_{1.6}]-**1a** were detected ($\Delta G^\ddagger = 31 \text{ kcal mol}^{-1}$). Moreover, near-identical kinetic isotope
4 effects, *vide infra*, were obtained for hydrolysis of **1a** at 0.5 M and at 9.1 M H₂O, above and
5 below the rate plateau, suggestive of mechanistic continuity. Aqueous THF forms non-ideal
6 mixtures,¹³ and by inclusion of a higher-order term for the water activity (a_w)¹⁴ the kinetic
7 dichotomy is resolved (Figure 2b). The resulting correlation ($k_0 = k'a_w^{2.8}$) suggests rate-
8 limiting attack of **1a** by water clusters (H₂O)_{*n*}, with average *n* = 2.8. The linear free energy
9 relationship for neutral hydrolysis ($\log(k_X/k_H) = 0.8\sigma$; 9.1 M H₂O) indicates moderate charge
10 accumulation at the aromatic ring, as for example in a partially-developed boronate anion.

11 *3. Kinetic Isotope Effects (KIEs)*. Further information on the sites of attack of **1a** (at C versus
12 B) by OH⁻, (H₂O)_{*n*} and H₂O/H⁺ during the rate-limiting events was deduced from KIEs.
13 Heavy-atom KIEs were determined by double-labelling, analysing [¹H₄] / [²H₄] ratios in
14 [*aryl*-²H_{*n*}(B,C,N)]-**1a** mixtures ($\Delta\delta_F = 0.56 \text{ ppm}$) as a function of fractional conversion. First-
15 order competitive rates (k_{rel}) were extracted by non-linear regression, then corrected for
16 independently-determined ²H-KIEs, to yield ^{10/11} k_B , ^{12/13} k_C and ^{14/15} k_N , under base, neutral and
17 acid conditions, Figure 4a-d.

18 For basic hydrolysis (k_{OH^-}), syringe-pump addition of aq. NaOH, *via* a submerged narrow bore
19 needle into a vigorously stirred solution of **1a** (10 mM), ensured reactions proceeded in a
20 basic aqueous-organic emulsion, prior to phase-separation. The KIE (^{12/13} $k_C = 1.049$; Figure
21 4b) together with the rate-law, indicates that a carbonyl group in **1a** is attacked by hydroxide
22 in the rate-determining step, without direct involvement of either B or N. The outcome for
23 acid-catalysed hydrolysis was analogous (^{12/13} $k_C = 1.041$, Figure 4c), indicative of rate-
24 limiting ester hydrolysis (k_{H^+}), albeit much less efficient ($k_{\text{H}^+} / k_{\text{OH}^-} = 1 \times 10^{-5}$).



1

2 **Figure 4 | Kinetic isotope effects (KIEs) for Ar-BMIDA (1a) hydrolysis.** (a) outline of methodology allowing KIE
 3 values to be extracted by a standard pseudo first-order competition model; heavy atom KIEs shown are those
 4 *after* correction for aryl deuteration,^{15,16} $\text{net-}\sigma_{\text{D}} = -6.3(\pm 0.15) \times 10^{-3}$, and competing processes ($k_{\text{H}^+} + k_0$). (b) Fast
 5 hydrolysis: substoichiometric aq. NaOH added to vigorously stirred solutions of **1a** (10 mM) to attain a suitable
 6 span of fractional conversions. Hydrolysis post phase-separation inhibited by addition of anhydrous MgSO₄. (c)
 7 Acid hydrolysis (1M HCl) analysed in situ. (d) Neutral hydrolysis analysed in situ. Identical KIES ($\Delta \leq \pm 0.002$)
 8 were obtained with 0.5 M H₂O. (e) Proton inventory conducted with **1a** in THF/L₂O (9.1 M, L = H, D). The net
 9 solvent KIE ($\chi_{\text{D}} = 1$) increases from 1.4 to 2.0 as $[\text{D}_2\text{O}]$ is decreased from 9.1 to 0.5 M.

10

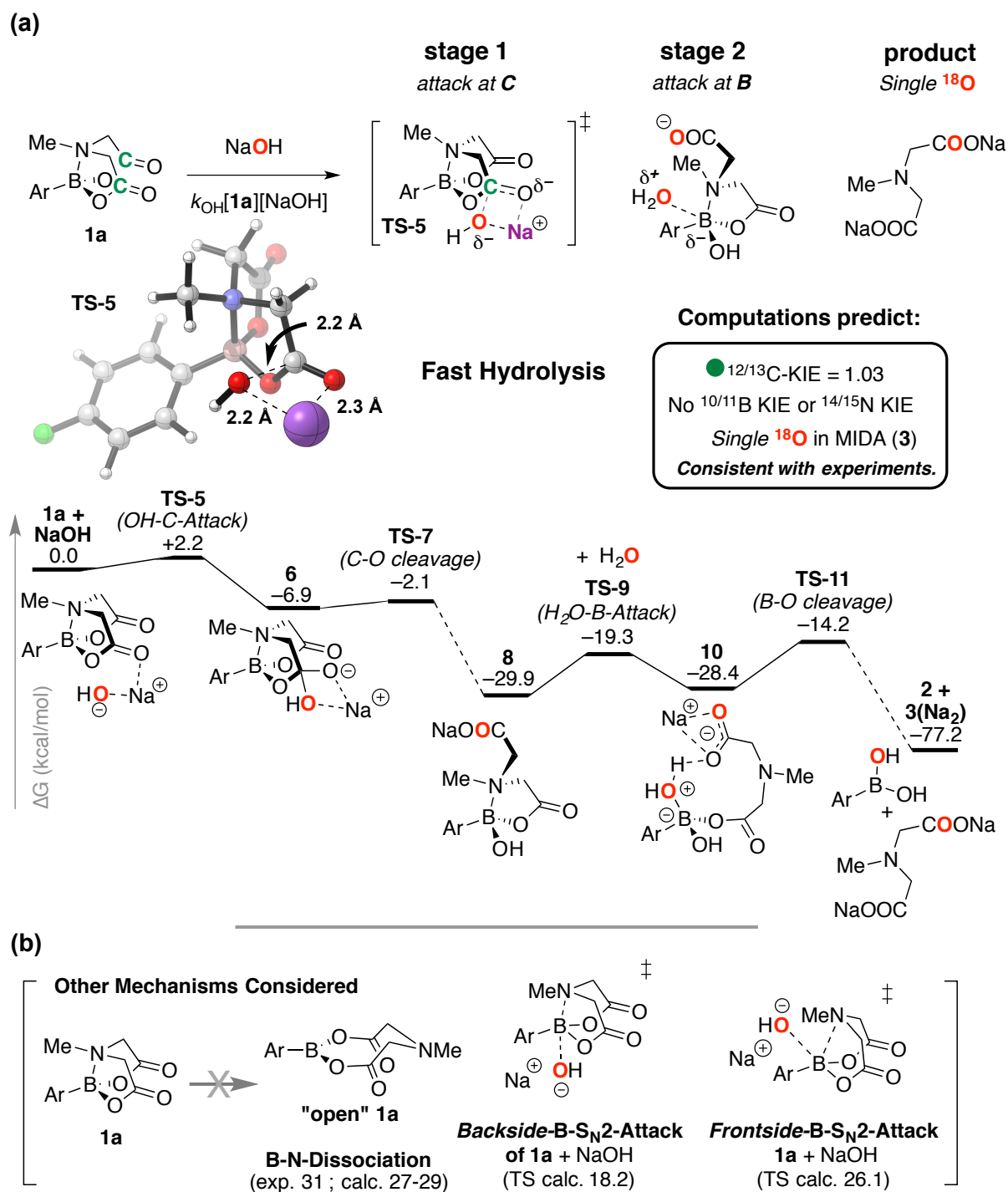
11 For neutral hydrolysis (k_0), the KIEs ($^{10/11}k_{\text{B}} = 1.032$, $^{14/15}k_{\text{N}} = 1.017$; Figure 4d) are
 12 complementary to those for the acid/base mechanisms, with no KIE detected at carbon.
 13 Proton inventory¹⁷ (Figure 4e) for neutral hydrolysis (k_0) in H₂O/D₂O/THF identified
 14 simultaneous primary ($k_{\text{H/D}} = 1.59$) and secondary ($k_{\text{H/D}} = 0.84$) KIEs; the effect of
 15 deuteration on the water activity in the neutral reaction (k_0) is expected to be negligible.¹⁸ The
 16 three normal primary KIEs (k_{H} , k_{B} , k_{N}) indicate that an O-H bond in the attacking water
 17 cluster, (H₂O)_n, is cleaved in the rate-determining event, and that the B-N bond, not the
 18 carbonyl unit, in **1a** is involved in this process. The inverse secondary $k_{\text{H/D}}$ arises from
 19 changes in solvation and H-bonding of the residual (non-transferred) water proton(s).¹⁹

1

2 **Discussion**

3 *4. Pathways for hydrolysis.* The data reported above allow a large number of mechanistic
4 possibilities to be ruled out. The unassisted cleavage of B-N to generate "open-**1a**" (Figure
5 3c) is 6-12 kcal mol⁻¹ greater in energy than the experimentally determined hydrolysis rates
6 (k_{OH} , k_0 , and k_{H^+}) thus eliminating S_N1-like pathways. Processes consistent with the rate-
7 limiting events are attack of **1** at the carbonyl carbon by OH⁻ (k_{OH}) or H⁺/H₂O (k_{H^+}), and at
8 the B-N unit by water (k_0). The slow (k_{H^+}) or undetected (k_{OH} ; k_0), rates of ^{16/18}O-exchange in
9 **1a** are inconclusive as the oxygen atoms in the tetrahedral intermediates remain inequivalent,
10 irrespective of proton exchange rates.²⁰ Nonetheless, in none of the hydrolyses were
11 intermediates detected by NMR (¹H, ¹⁹F, ¹¹B), or UV (isosbestic points) suggesting that after
12 rate-limiting addition of (H⁺/H₂O), OH⁻, or (H₂O)_n, hydrolytic evolution to the boronic acid
13 (**2a**) and MIDA ligand (**3**) is rapid. Substantial additional insight to the 'fast-release' (k_{OH}) and
14 'slow-release' (k_0) pathways relevant to coupling conditions^{2,3} was gained by computations,
15 using Gaussian 09²¹ at the M06-2X²²/6-31G*²³/PCM²⁴(THF) level of theory. In Figures 5a
16 and 6a we provide a summary of the key stages of the two pathways identified. Some of the
17 other mechanisms we considered are also given (Figures 5b/6b), with full details in the
18 Supporting Information.

19 *The Fast-Release (k_{OH}) pathway:* the minimum energy pathway begins with the rate-limiting,
20 irreversible, attack by hydroxide at one of the two ester carbonyls in **1a** (C-Attack **TS-5**, ΔG^\ddagger
21 = 2.2 kcal/mol, Figure 5a). Fast ($\Delta G^\ddagger \leq 5$ kcal/mol), highly exothermic, irreversible collapse
22 of the now tetrahedral carbonyl carbon (**TS-7**) generates ring-opened intermediate **8** ($\Delta G = -$
23 29.9 kcal/mol). Due to the presence of a pendent carboxylate and increased lability of the B-
24 N bond, **8** is substantially more prone to hydrolysis than neutral MIDA **1a**. Stage 2 hydrolysis
25 proceeds via attack of **8** at the boron by water (**TS-9**, $\Delta G^\ddagger = 10.6$ kcal/mol), leading to **10**,
26 and thus to final products (**2** + **3**) via B-O bond cleavage and ionization/salt formation.
27 NaOH-mediated rate-limiting C=O attack is consistent with experiment (computed ^{12/13} k_C
28 KIE 1.03), the low sensitivity to aryl substituents ($\rho = 0.5$), and the absence of experimentally
29 observable ^{14/15} k_N or ^{10/11} k_B KIEs.



1

2 **Figure 5 | Fast-release Hydrolysis (k_{OH}).** (a) Summary key computational data for hydrolysis of **1a** via C-O

3 cleavage (TS-5). Computed minimum-energy pathway and experimental data are fully self-consistent.

4 Nonetheless, these computed results do not resort to exhaustive, time-dependent sampling, and should thus

5 be taken only as a model of the processes taking place in solution. (b) Other key processes considered.

6

7 *The Slow-Release (k_0) pathway:* The minimum energy pathway begins with the rate-limiting

8 insertion of water into a stretching, but not cleaved, B-N bond (Frontside-B-S_N2-Attack, TS-

9 **12**, +25.7 kcal/mol), Figure 6a.

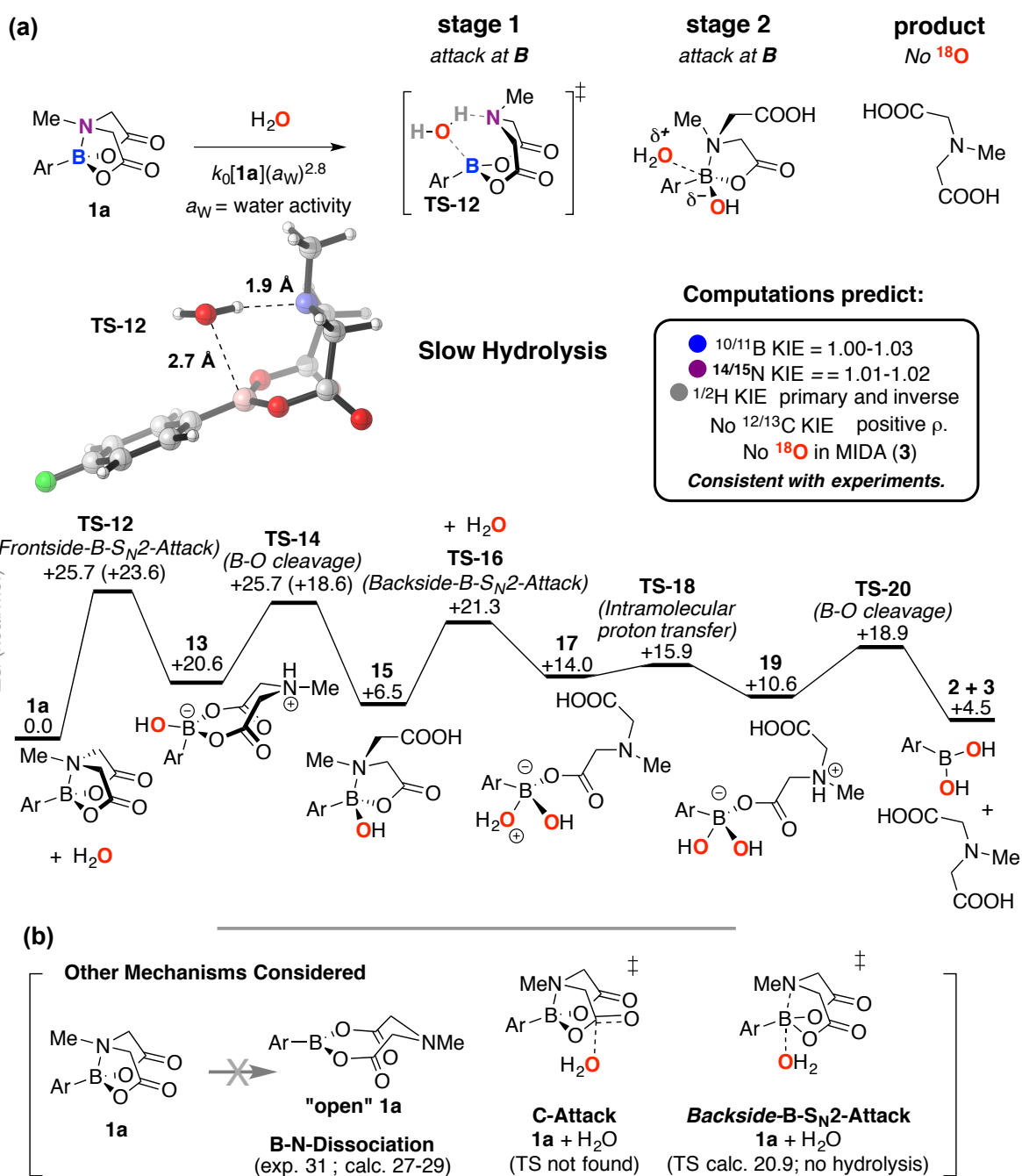


Figure 6 | Slow-release Hydrolysis (k_0). (a) Summary key computational data for hydrolysis of **1a** via B-N bond cleavage (**TS-12**). (b) Other key processes considered. For caveats see caption to Figure 5.

At higher water concentrations, B-N cleavage by $(\text{H}_2\text{O})_n$, $n = 1,2,3$ has similar free energy barriers, and KIEs for these were computed with a range of levels of theory.²⁵ The best quantitative agreement was found in a late transition state using M06L/6-311++G**. As the B-O bond is formed to a great degree, with significant proton transfer to the nitrogen, there is negative charge accumulation at B (ρ 0.4 to 1.0). Stage 2 hydrolysis again involves a ring-

1 opened intermediate (**15**)_m, which via intramolecular deprotonation boron-coordinated water
2 (**TS-18**), rapidly leads to complete hydrolysis. Rate-limiting B-N cleavage by H₂O is
3 consistent with experiment (computed KIEs ^{14/15}k_N 1.01, ^{10/11}k_B 1.03, ^{1/2}k_H 0.9 and 1.4) the
4 sensitivity to aryl substituents (ρ = 0.8), and the absence of experimentally observable ^{12/13}k_C
5 KIE.

6 *Other Mechanisms Considered and Additional Considerations:* As detailed in the Supporting
7 Information, we also extensively probed alternative mechanisms for fast and slow hydrolysis,
8 at both the first- and second-stages. For stage one fast hydrolysis (Figure 5b), B-N bond
9 cleavage by backside-B-S_N2 or frontside-B-S_N2 attack of hydroxide is disfavoured by ≥16
10 kcal/mol. The barrier for stage two attack of **8** by hydroxide, at carbon or at boron (the latter
11 being slightly favoured ΔΔG[‡] 2.2 kcal mol⁻¹) is also prohibitively high. The kinetics, KIEs,
12 and ¹⁸O incorporations, indicate that a similar overall pathway (attack of a C=OH⁺
13 intermediate by H₂O, then attack at B) operates under acid catalysis (k_{H+}). Slow hydrolysis
14 (k₀) proceeds without exogenous acid or base, and no transition state for H₂O attack at carbon
15 (C-Attack, Figure 6b) could be located. Nonetheless, simple esters do slowly hydrolyse in
16 pure water (ΔG[‡] = 21-28 kcal/mol),²⁶ a process for which water chains,^{26,27} and water
17 autoionisation mechanisms (ΔG[‡] = 23.8 kcal/mol)²⁸ have been proposed. Thus, irrespective
18 of whether hydrolytic cleavage (k₀) of B-N in **1a** (ΔG[‡] = 23.6 kcal/mol) involves transient
19 water autoionisation, or concerted transfer (as in **TS-12**), appropriate dynamic fluctuations of
20 water chains²⁹ will be required to facilitate it. An alternative mechanism for stage one slow-
21 hydrolysis involves Backside-B-S_N2-Attack (Figure 6b) leading to a weakly bound complex,
22 from which water-deprotonation by carboxylate cleaves the B-O bond. This is computed to
23 result in a large primary KIE (^{1/2}k_H ≈ 3.8), inconsistent with experiment (Figure 4e). Overall,
24 the differing rates and sites of first stage attack (OH⁻ at C in **TS-5**, versus H₂O at B-N in **TS-**
25 **12**) can be rationalised by: i) hydroxide being much more nucleophilic than water (k_{OH}[OH]
26 >> k₀[H₂O]ⁿ); ii) the anionic charge from attacking hydroxide being delivered to an
27 electrophilic site (C=O); and iii) that B-N in **1** can simultaneously function as a Bronsted base
28 and Lewis acid to provide a 'receptor' for activating water. After the stage one rate-limiting
29 processes (k_{OH}, k₀ and k_{H+}), all pathways converge, albeit with different net charges, via ring-
30 opened intermediates (e.g. **8** and **15**) where intramolecular activation can assist stage two
31 hydrolysis, at boron.

32

1 *5. MIDA boronate hydrolysis under conditions of application.*

2 We have identified two general mechanisms (ester versus B-N cleavage) for hydrolysis of **1a**
3 operating under basic, neutral and acidic conditions. Of these, k_{OH} is by far the most efficient,
4 becoming the major pathway when $[\text{NaOH}] \geq 3 \mu\text{M}$. At concentrations used for synthesis, the
5 conditions for 'fast' and 'slow' release, Figure 1, result in separation into aqueous and organic
6 phases. Maintaining high rates of fast release (k_{OH}) is assisted by generation of a transient
7 emulsion, usually attained by vigorous agitation during slow dispersive addition of aq.
8 NaOH. In the fully phase-separated medium, boronate (**1a**) undergoes slow hydrolysis in the
9 bulk organic-aqueous upper phase, the rate being mildly dependent on stirring and mass-
10 transfer rates between phases, and the activity of the water (a_{w}) in the bulk organic phase.
11 This detailed mechanistic understanding of the rate-limiting events for both hydrolysis
12 pathways, and the physicochemical factors that govern their partitioning, enable
13 rationalisation of many of the phenomenological observations previously recorded with the
14 MIDA platform.

15 The more than three orders of magnitude difference in rate attainable for fast versus slow
16 hydrolysis results from the distinct mechanisms underlying these processes. The remarkable
17 insensitivity of these rates to the structure of the appended organic fragment is consistent with
18 minimal charge build-up at the boron center during attack at the carbonyl during fast release
19 and the presence of a common intramolecular base for facilitating insertion of water into the
20 N-B bond during slow-release. The stability of MIDA boronates in anhydrous solvents in the
21 presence of inorganic bases, essential for iterative coupling, is consistent with the
22 requirement for substantial water in the organic phase in order to promote neutral hydrolysis.
23 MIDA boronates bearing exceptionally lipophilic organic fragments induce accelerated
24 phase-separation when treated with NaOH, resulting in resulting in more rapid switching to
25 neutral hydrolysis and thus significantly extended reaction times for their complete
26 hydrolysis. The slow-release cross-coupling of boronic acids proceeds via MIDA boronate
27 hydrolysis in the upper aqueous-organic phase, while the inorganic base remains in the lower
28 aqueous phase. The rates of hydrolysis under these slow-release conditions are highly reliable
29 because the activity of water in THF,¹² and in dioxane,³⁰ is approximately constant ($a_{\text{w}} \approx 0.8$ –
30 1.0) above concentrations of 3.0 M. The stability of MIDA boronates to many acidic
31 conditions is consistent with their substantially slower rates of hydrolysis observed at low
32 versus high pH.

1 This advanced mechanistic understanding also stands to practically enable more
2 effective and widespread utilisation of MIDA boronates in synthesis. The rates of “slow-
3 release” of unstable boronic acids from their MIDA boronate counterparts³ can now be
4 rationally tuned by simply varying the conditions to increase or decrease the contribution of
5 basic vs. neutral hydrolysis mechanisms. Using more organic soluble hydroxide salts should
6 further homogenise the rates of fast hydrolysis of even highly lipophilic MIDA boronate
7 intermediates thus enabling standardization of conditions and thus automation. Increasing the
8 dielectric constant of aqueous phases during reaction work-ups should help avoid undesired
9 hydrolysis of MIDA boronates in organic phases and thereby enable more effective building
10 block syntheses. Using buffered HPLC eluents should maximise MIDA boronate stability
11 during analysis and purifications. This same understanding forms the basis for rational design
12 of new MIDA boronate analogues where both modes of hydrolysis are deliberately retarded
13 or accelerated by modifications to the iminodiacetic acid backbone. Such ligands stand to
14 broadly enable advanced applications of organoboron compounds in synthesis, including
15 expanding the range of reaction conditions compatible with complex building block
16 construction and iterative assembly, opening new opportunities for selective boron
17 deprotections and even one-pot pre-programmed iterative synthesis, and facilitating a
18 transition in automation platforms from batch to flow chemistry. Such efforts can also now be
19 guided by quantitatively tracking the relative contributions of the mechanisms of hydrolysis
20 (k_{OH} / k_0) simply by determining the ¹⁸O-incorporation in the cleaved ligands (**3**) when
21 conducting reactions in labelled water. These advances stand to powerfully assist in the
22 development of a more general and automated approach for small molecule synthesis.

23

24 **Methods**

25

26 **General.** DFT calculations of MIDA boronate solvolysis in basic and neutral aqueous THF were conducted at
27 the M06-2X/6-31G* level of theory with solvation using a polarized continuum model (PCM) for THF. The
28 MIDA boronates were prepared from the corresponding boronic acid (**2a**, ²H₄-**2a**, ¹⁰B-**2a**, ¹¹B-**2a**) and *N*-
29 methyliminodiacetic acid (**3**, ¹⁵N-**3**, ¹³C₂-**3**) using standard procedures,² and purified *via* silica-gel column
30 chromatography (Et₂O/MeCN 4:1) then recrystallisation (MeCN-Et₂O). See supporting information for full
31 details.

32

33 **Kinetics of MIDA Boronate Solvolysis in Basic Organic Emulsion (Fast Release).** A stopped-flow system
34 (TgK Scientific) was employed to deliver solutions of the isolated reactants (**1a**, 0.5 to 2.5 mM and NaOH, 2.5-

1 7.5 mM) in aqueous THF ($[\text{H}_2\text{O}] = 9.1 \text{ M}$) in 1 : 1 volume ratio, via thermostatted reagent lines, into a fused-
2 silica UV-vis cuvette (pathlength 10 mm) with integral pre-mixer (dead-time < 8 msec). Spectra were collected
3 at 10 msec intervals on an Ocean Optics USB4000 detector and data processed (Kinetic Studio; TgK Scientific)
4 to afford the rate of change in absorbance (A) at 264 nm. To determine heavy atom KIEs, samples of $[\text{aryl-}^2\text{H}_n]$ -
5 **1a**, as an approximately 1: 1 mixture of $n = 0$ and $n = 4$, with isotopically labelled MIDA boronate moieties
6 ($^{10}\text{B}/^{11}\text{B}/^{13}\text{C}_2/^{15}\text{N}$), in one or other sample, were dissolved in 50 mL THF to give a total concentration of 10 mM.
7 4,4'-bis-(CF₃)-biphenyl was added as an internal standard. Aliquots (5 mL) were then transferred to round-
8 bottom flasks, and vigorously stirred (> 1000 rpm) as 1 mL of an aqueous solution of NaOH was added through
9 a narrow-bore needle via syringe pump over 5 minutes. A series of NaOH concentrations (1-30 mM) were
10 delivered to the sequence of aliquots to attain a suitable range of fractional conversions under metastable locally
11 emulsified conditions. Immediately after addition of the requisite volume of NaOH solution, the reactions were
12 chilled in ice, and sufficient anhydrous MgSO₄ added to inhibit further hydrolysis (k_{OH} and k_0). The solutions
13 were concentrated (40 °C, 150 mBar) to approximately 0.5 mL and the isotope ratio and conversion analysed by
14 ¹⁹F NMR.

15

16 **Kinetics of Solvolysis of MIDA Boronate **1a** in the Absence of Exogenous Base (Slow Release).** Reactions
17 were conducted in 5 mm NMR tubes kept at constant temperature ($\pm 0.5 \text{ }^\circ\text{C}$) in a thermostatted environment. A
18 0.6- x mL aliquot of a stock solution of MIDA boronate **1a** in THF containing 4-CF₃-bromobenzene as internal
19 standard, followed by x mL of aqueous THF, were added to the tube to establish final concentrations of 0.1 M
20 **1a** and 9.1 M H₂O. The sample was vigorously mixed, a sealed glass capillary containing DMSO-*d*₆ added, the
21 NMR tube sealed (J-Young valve) and then inserted into NMR spectrometer (Bruker Advance; 376.3 MHz ¹⁹F).
22 After the spectrometer had been ²H-frequency-locked to the DMSO-*d*₆, a series of ¹⁹F NMR spectra were
23 recorded. The spectra were processed, as a block, and the integration of the ¹⁹F NMR signals (inter-FID delays >
24 $5 T_1$) for the internal standard, **1a** and **2a** used to calculate concentrations. The pseudo-first order rate constant
25 (k_{obs}) was obtained from plots of $\ln([\mathbf{1a}]_0/[\mathbf{1a}]_t) = k_{\text{obs}} \cdot t$; correlations were generally excellent (r^2 typically \geq
26 0.99). Reactions were conducted across a wide range of other initial water concentrations (0.5 to 20.0 M), and
27 with mixtures of H₂O/D₂O; $[\text{L}_2\text{O}] = 9.1 \text{ M}$. The same procedure was employed to determine heavy atom KIEs,
28 except that $[\text{aryl-}^2\text{H}_n]$ -**1a**, as an approximately 1: 1 mixture of $n = 0$ and $n = 4$; with isotopically labelled MIDA
29 boronate moieties ($^{10}\text{B}/^{11}\text{B}/^{13}\text{C}_2/^{15}\text{N}$), in one or other sample, were employed.

30

31 References

- 32 1. Li, J., Grillo, A. S., & Burke, M. D. From synthesis to function via iterative assembly of *n*-
33 methyliminodiacetic acid boronate building blocks. *Acc. Chem. Res.* **48**, 2297–2307 (2015).
- 34 2. Gillis E. P., & Burke M. D. A simple and modular strategy for small molecule synthesis: iterative
35 Suzuki–Miyaura coupling of B-protected haloboronic acid building blocks. *J. Am. Chem. Soc.* **129**, 6716–
36 6717 (2007).
- 37 3. Knapp, D. M., Gillis, E. P., & Burke, M. D. A general solution for unstable boronic acids: slow-release
38 cross-coupling from air-stable MIDA Boronates. *J. Am. Chem. Soc.* **131**, 6961–6963 (2009).
- 39 4. Lennox, A. J. J.; Lloyd-Jones, G. C. Organotrifluoroborate hydrolysis: boronic acid release mechanism and
40 an acid-base paradox in cross-coupling. *J. Am. Chem. Soc.* **134**, 7431–7441 (2012).

- 1 5. Woerly, E. M., Roy, J., & Burke, M. D. Synthesis of most polyene natural product motifs using just 12
2 building blocks and one coupling reaction. *Nature Chem.* **6**, 484–491 (2014).
- 3 6. Li, J., et al. Synthesis of many different types of organic small molecules using one automated process.
4 *Science* **347**, 1221–1226 (2015).
- 5 7. Dick, G. R., Woerly, E. M., & Burke, M. D. A General solution for the 2-pyridyl problem. *Angew. Chem.*
6 *Int. Ed.* **51**, 2667–2672 (2012).
- 7 8. Fyfe, J. W. B., Seath, C. P., & Watson, A. J. B. Chemoselective boronic ester synthesis by controlled
8 speciation. *Angew. Chem. Int. Ed.* **53**, 12077–12080 (2014).
- 9 9. Li, J., & Burke, M. D. Pinene-derived iminodiacetic acid (PIDA): a powerful ligand for stereoselective
10 synthesis and iterative cross-coupling of $c(sp^3)$ boronate building blocks. *J. Am. Chem. Soc.* **133**, 13774–
11 13777 (2011).
- 12 10. Grob, J. E., et al. One-pot C–N/C–C cross-coupling of methyliminodiacetic acid boronyl arenes enabled by
13 protective enolization. *Org. Lett.* **14**, 5578–5581 (2012).
- 14 11. Gillis, E. P., & Burke, M. D. Multistep synthesis of complex boronic acids from simple MIDA boronates.
15 *J. Am. Chem. Soc.* **130**, 14084–14085 (2008).
- 16 11. Butters, M., Harvey, J. N., Jover, J., Lennox, A. J. J., Lloyd-Jones, G. C. & Murray, P. M. Aryl
17 trifluoroborates in Suzuki–Miyaura coupling: the roles of endogenous aryl boronic acid and fluoride.
18 *Angew. Chem. Int. Ed.* **49**, 5156–5160 (2010).
- 19 12. Bender, M. L., & Thomas, R. J. The concurrent alkaline hydrolysis and isotopic oxygen exchange of a
20 series of *p*-substituted methyl benzoates. *J. Am. Chem. Soc.* **83**, 4189–4193 (1961).
- 21 13. Blandamer, M. J., Engberts, J. B. F. N., Gleeson, P. T. & Reis, J. C. R. Activity of water in aqueous
22 systems; a frequently neglected property. *Chem. Soc. Rev.* **34**, 440–458 (2005).
- 23 14. Treiner, C., Bocquet, J.-F., & Chemla, M. Seconds coefficients du viriel des melanges eau-
24 tetrahydrofurane (THF) influence sur les coefficients d'activite de l'eau et du THF a 25 °C. *J. Chim.*
25 *Phys.-Chim. Biol.* **70**, 72–79 (1973).
- 26 15. Perrin, C. L., & Dong, Y. Secondary deuterium isotope effects on the acidity of carboxylic acids and
27 phenols. *J. Am. Chem. Soc.* **129**, 4490–4497 (2007).
- 28 16. Pehk, T., Kiirend, E., Lippmaa, E., Ragnarsson, U., & Grehn, L. Determination of isotope effects on acid-
29 base equilibria by ^{13}C NMR spectroscopy. *J. Chem. Soc., Perkin Trans. 2*, 445–450 (1997).
- 30 17. Krishtalik, L. I. On the theory of the 'Proton Inventory' method. *Mendeleev Commun.* **3**, 66–67 (1993).
- 31 18. Glew, D. N., & Watts, H. Aqueous Non-electrolyte Solutions. Part XII. Enthalpies of mixing of water and
32 deuterium oxide with tetrahydrofuran. *Can J. Chem.* **51**, 1933–1940 (1973).
- 33 19. Schowen, R. L. The use of solvent isotope effects in the pursuit of enzyme mechanisms. *J. Label. Compd.*
34 *Radiopharm.* **50**, 1052–1062 (2007).
- 35 20. Bender, M. L., Matsui, H., Thomas, R. J., & Tobey, S. W. The concurrent alkaline hydrolysis and isotopic
36 oxygen exchange of several alkyl benzoates and lactones. *J. Am. Chem. Soc.* **83**, 4193–4196 (1961).
- 37 21. M. J. Frisch, et al. Gaussian, Inc.: Wallingford, CT, 2009. See Supporting Information for full authorship.
- 38 22. Zhao, Y. & Truhlar, D. G. The M06 suite of density functionals for main group thermochemistry,
39 thermochemical kinetics, noncovalent interactions, excited states, and transition elements: two new
40 functionals and systematic testing of four M06-class functionals and 12 other functionals. *Theor. Chem.*
41 *Acc.* **120**, 215–241 (2008).
- 42 23. Hariharan, P. C. & Pople, J. A. The influence of polarization functions on molecular orbital hydrogenation
43 energies. *Theoret. Chim. Acta* **28**, 213–222 (1973).
- 44 24. Miertus, S., Scrocco, E. & Tomasi, J. Electrostatic interaction of a solute with a continuum. A direct
45 utilization of AB initio molecular potentials for the prevision of solvent effects. *Chem. Phys.* **55**, 117–129
46 (1981).

- 1 25. Beno, B. R., Houk, K. & Singleton, D. A. Synchronous or asynchronous? An “experimental” transition
2 state from a direct comparison of experimental and theoretical kinetic isotope effects for a Diels-Alder
3 reaction. *J. Am. Chem. Soc.* **118**, 9984–9985 (1996).
- 4 26. Guthrie, J. P. Hydration of carbonyl compounds, an analysis in terms of multidimensional Marcus Theory.
5 *J. Am. Chem. Soc.* **122**, 5529–5538 (2000).
- 6 27. Guthrie, J. P. & Pitchko, V. Hydration of carbonyl compounds, an analysis in terms of no barrier theory:
7 prediction of rates from equilibrium constants and distortion energies. *J. Am. Chem. Soc.* **122**, 5520–5528
8 (2000).
- 9 28. Gunaydin, H. & Houk, K. N. Molecular dynamics prediction of the mechanism of ester hydrolysis in
10 water. *J. Am. Chem. Soc.* **130**, 15232–15233 (2008).
- 11 29. Geissler, P. L., Dellago, C., Chandler, D., Hutter, J., & Parrinello, M. Autoionization in liquid water.
12 *Science* **291**, 2121–2124 (2001).
- 13 30. Besbes, R., Ouerfelli, N. & Latrous, H. Density, dynamic viscosity, and derived properties of binary
14 mixtures of 1,4 dioxane with water at T=298.15 K. *J. Mol. Liq.* **145**, 1–4 (2009).

15

16 **Acknowledgements**

17 GCLJ is an ERC Advanced Investigator. The research leading to these results has received
18 funding from the European Research Council under the European Union's Seventh
19 Framework Programme (FP7/2007-2013) / ERC grant agreement n° [340163], and the U.S.
20 National Institutes of Health. GCLJ and JAG thank CONACYT and The University of
21 Edinburgh for generous support. PHYC is the Bert and Emelyn Christensen professor of
22 OSU, and gratefully acknowledges financial support from the Stone family and the National
23 Science Foundation (NSF, CHE-1352663). KNH is Saul Winstein Chair in Organic
24 Chemistry at UCLA and acknowledges generous financial support from the US National
25 Science Foundation (CHE-1059084). OMO acknowledges Tartar research support. OMO and
26 PHYC also acknowledge computing infrastructure in part provided by the NSF Phase-2 CCI,
27 Center for Sustainable Materials Chemistry (NSF CHE-1102637).

28

29 **Author contributions**

30 Experimental work was conducted by JAG and GFM. Computational work was conducted by
31 OMO, NR, PHYC and AGL.

32

33 **Additional information**

34 Full experimental procedures, computational details, as well as experimental data and
35 computational discussion, are provided in the supporting information.

1

2 **Competing financial interests**

3 The University of Illinois has filed patent applications related to MIDA boronate chemistry,
4 and these have been licensed to REVOLUTION Medicines, a company for which MDB is a
5 founder and consultant.

6